PNAS RESEARCH ARTICLE | NEUROSCIENCE

Pathway-selective optogenetics reveals the functional anatomy of top–down attentional modulation in the macaque visual cortex

Janina Hüer[a,b,1], Pankhuri Saxena[a], and Stefan Treue[a,c,d,e]

Edited by Robert Desimone, Massachusetts Institute of Technology, Cambridge, MA; received March 18, 2023; accepted October 7, 2023

Spatial attention represents a powerful top–down influence on sensory responses in primate visual cortical areas. The frontal eye field (FEF) has emerged as a key candidate area for the source of this modulation. However, it is unclear whether the FEF exerts its effects via its direct axonal projections to visual areas or indirectly through other brain areas and whether the FEF affects both the enhancement of attended and the suppression of unattended sensory responses. We used pathway-selective optogenetics in rhesus macaques performing a spatial attention task to inhibit the direct input from the FEF to area MT, an area along the dorsal visual pathway specialized for the processing of visual motion information. Our results show that the optogenetic inhibition of the FEF input specifically reduces attentional modulation in MT by about a third without affecting the neurons' sensory response component. We find that the direct FEF-to-MT pathway contributes to both the enhanced processing of target stimuli and the suppression of distractors. The FEF, thus, selectively modulates firing rates in visual area MT, and it does so via its direct axonal projections.

frontal eye field | spatial attention | target enhancement | distractor suppression | motion processing

Significance

Visual attention is a top–down influence affecting sensory responses in visual areas that helps us to separate relevant from irrelevant information. How is this mechanism implemented in the brain? What are the underlying neural pathways? Our study identifies the direct axonal projection from the prefrontal to visual cortex as a key anatomical component. This pathway not only mediates the enhancement of attended but also the suppression of unattended information in the visual cortex.

The allocation of visual attention in primates is controlled by a network of cortical and subcortical areas (1–4). One of the most fundamental effects of attention is a modulation of firing rates in early and mid-level areas of the visual cortex (3, 5–8), specifically enhancing the sensory responses to attended and reducing the response to unattended stimulus locations and features. However, it is unknown how this modulation of firing rates arises and how the areas of the attentional network contribute to it.

Several brain areas have been identified to play critical roles during attention: the frontal eye field (9–11), the lateral intraparietal area (LIP) (12–16), as well as the subcortical superior colliculus (17–19), and the thalamic pulvinar nucleus (20, 21). Among these, the frontal eye field is regarded as the key area in the attentional modulation of cortical activity since none of the other areas has been shown to directly affect the attentional modulation of firing rates in the visual cortex.

FEF possesses direct axonal projections to extrastriate visual areas V4 and MT (22–24). Several studies in area V4 of the temporal visual pathway indicate that the FEF provides a feedback signal that mediates the differential attentional gain modulation of neuronal responses to attended and unattended sensory stimuli (10, 25–31). They show that microstimulation (10) or pharmacological activation (27) of FEF neurons enhances or suppresses V4 responses, effects similar to the effect of the allocation of spatial attention. In addition, several studies have found oscillatory synchronization between area FEF and V4 during attention in nonhuman primates (26, 28) and humans (30, 31). The most direct evidence for the role of FEF in modulating firing rates in visual areas stems from a study in which the prefrontal cortex of one hemisphere, including the FEF, was lesioned (29). This reduced the attentional modulation of neural activity in ipsilateral V4 compared to the attentional modulation in V4 of the nonlesioned hemisphere and increased the latencies of attentional effects. However, even though there is ample evidence for the role of FEF's impact on visual area V4, similar evidence is lacking for the dorsal visual pathway. Specifically, the effect of FEF feedback manipulation on area MT, an area crucial for visual motion processing and its attentional modulation, is unknown.

In addition, the studies mentioned above are not suited to discriminate a direct anatomical feedback from the FEF from the many indirect feedback connections from the FEF to extrastriate cortex. For this, it is crucial to conduct causal manipulations of components of the network. Inactivation studies, in general, can provide direct evidence for the contribution of an area because they inhibit the naturally occurring activity. In contrast, activation by electrical microstimulation or optogenetic excitation

Author affiliations: [a]Cognitive Neuroscience Laboratory, German Primate Center, Leibniz Institute for Primate Research, Göttingen 37077, Germany; [b]Ernst Strüngmann Institute for Neuroscience in Cooperation with Max Planck Society, Frankfurt 60528, Germany; [c]Faculty of Biology and Psychology, University of Göttingen, Göttingen 37073, Germany; [d]Leibniz-ScienceCampus Primate Cognition, Göttingen 37077, Germany; and [e]Bernstein Center for Computational Neuroscience, Göttingen 37073, Germany

Author contributions: J.H. and S.T. designed research; J.H. and P.S. performed research; J.H., P.S., and S.T. analyzed data; and J.H., P.S., and S.T. wrote the paper.

The authors declare no competing interest.

This article is a PNAS Direct Submission.

[1]To whom correspondence may be addressed. Email: jhueer@gwdg.de.

This article contains supporting information online at https://www.pnas.org/lookup/suppl/doi:10.1073/pnas.2304511121/-/DCSupplemental.

Published January 9, 2024.

introduces artificial activity within an area that does not necessarily resemble the naturally occurring activity. However, broad inactivation of potential source areas can affect all areas that are anatomically connected to the inactivated area and, in addition, can trigger adaption processes that compensate for the inactivation effects (16). Therefore, what is needed are small-scale causal manipulations, that avoid changes in the natural behavior of the animals and leave intact and unmodulated other neural pathways within the attentional network. In the last decade, the use of optogenetics in nonhuman primates has become widespread, and it offers new possibilities to dissect the causal interactions within cortical networks (32–34).

In this study, we used pathway-selective optogenetics (33, 35) to selectively manipulate the axonal projections from the FEF to visual area MT to determine whether the FEF affects the attentional modulation of firing rates in MT via this direct pathway. In a previous study, we have shown that injection of a viral vector into the FEF leads to the incorporation of opsins into the axonal membrane of FEF neurons projecting to area MT (36). FEF feedback projections were found in layer I and layer V/VI in area MT. In the current study, we used the same viral construct containing the sequence for an inhibitory opsin to inhibit these FEF feedback projections to area MT by laser stimulation in MT.

We injected a viral vector (AAV5-αCaMKII-eNpHR3.0-mCherry) into the FEF of two rhesus macaques [an extended histological analysis of one of the monkeys of this study can be found in our previous study (36)] and optically stimulated the axonal projections from the FEF to area MT locally within area MT while the animals performed a spatial attention task (Fig. 1 *C*–*F*). We recorded single-unit activity in area MT and limited the laser stimulation to the proximity of the recorded neurons, assuming that the FEF-to-MT-projection is retinotopically organized and that the major FEF input signal to an MT neuron is localized to its vicinity. In addition, we wanted to avoid large changes in the behavior of the animal to keep neural activity outside of area MT as unchanged as possible.

The experiment allowed us to address three open questions. The first is whether the FEF plays a role in the attentional modulation of firing rates of area MT neurons. The second question we address is whether the direct axonal projection from the FEF to visual areas alone is sufficient for a significant contribution to the modulation of firing rates during attention. The third question our design allowed to address is whether the FEF contributes to both the enhanced processing of attended stimuli and the suppression of distractors within visual areas.

Results

To address our three central questions, we recorded single-cell activity in area MT in combination with laser stimulation of FEF axonal projections after viral vector injection into the FEF of two rhesus monkeys. For each neuron, we recorded neuronal responses during two attention conditions (AttIN and AttOUT), combined with two laser conditions (noLaser and laser) (Fig. 1 *A* and *B*). Comparing the attentional modulation without and with laser stimulation allowed us to test our hypothesis that the direct FEF input to MT neurons carries an attentional control signal, modulating specifically the changes in MT neuronal responses when alternating the location of spatial attention, leaving the sensory response components unaffected.

Time Course of Firing Rates and Attentional Modulation. In the AttIN condition, the animals were required to attend to a random dot pattern (RDP) presented inside the receptive field (RF) of the neuron under study and moving in the neuron's preferred direction (Fig. 1 *A* and *B*). In the AttOUT condition, the animals directed their spatial attention to another RDP, placed outside the RF. Such a task combination has been shown to be very suitable to document the effect of spatial attention on neurons in area MT (37, 38). And indeed, for the large majority (118 of 138) of the recorded neurons the attentional modulation index was positive, meaning that firing rates were higher in the AttIN condition than in the AttOUT condition. To evaluate our hypothesis of a causal role of the direct input from the FEF in this attentional influence on MT responses, we focused our analysis on these 118 neurons. Fig. 2 shows the average time course of responses for two example neurons for the four task conditions, confirming modulation of sensory responses in area MT by the allocation of spatial attention in the absence of laser stimulation. Laser stimulation reduced the attentional modulation of these neurons.

The Fig. 3*A* shows the population average time course for the four conditions. For each neuron, we calculated an attentional modulation index (AMI) separately for the two laser conditions (noLaser and laser) based on the average firing rate for the steady-state response period (320 ms to 1000 ms after RDP onset). To estimate the effect of laser stimulation on the population level, we compared the distributions of attentional modulation indices (Fig. 3*B*).

We found a median increase of firing rates with attention by 19.4% without laser stimulation (AMI: 0.089). With laser stimulation, this median attentional modulation dropped to 13.6% (AMI: 0.064). Inhibition of the projection from the FEF to area MT, hence, decreased attentional modulation by 30% (Wilcoxon signed-rank test, $P < 0.001$). Overall, the attentional modulation index of 61% (72/118) of our neurons was decreased with laser stimulation, while it was increased for 39% (46/118) of the neurons.

Effects of Laser Stimulation on Target and Distractor Processing. The effect of spatial attention on the representation of the visual input is a combination of an enhanced response to stimuli at attended locations and a reduced response to stimuli at unattended locations (39, 40). To determine whether the FEF input contributes to both components of this push–pull modulation, we looked at how laser stimulation changes firing rates in the two attention conditions (AttIN and AttOUT). Specifically, we were wondering whether inhibition of the FEF input via laser stimulation would both reduce firing rates in the AttIN condition (i.e., diminish the attentional enhancement of the attended stimulus' representation) and increase firing rates in the AttOUT condition (i.e., diminish the attentional reduction of the unattended stimulus' representation).

Consistent with our hypothesis, we found that the observed reduction in attentional modulation from 19.4 to 13.6% by laser stimulation is a combination of a significantly decreased firing rate in the AttIN condition (−2.1% on average, Wilcoxon signed-rank test, $P < 0.05$, Bonferroni–Holm corrected for multiple comparisons) and a significantly increased firing rate in the AttOUT condition (+3.4% on average, Wilcoxon signed-rank test, $P < 0.05$, Bonferroni–Holm corrected).

Classification of Neuronal Cell Type Based on Waveform Duration. Previous studies have found differences in how attention affects different cell types of neurons (41–44). Therefore, we used the same approach as the previous studies and classified neurons based on their waveform duration. We found a bimodal distribution with marginal significance (Hartigan's dip test: $P = 0.059$, *SI Appendix*, Fig. S2), with 63 of 115 (55%) neurons

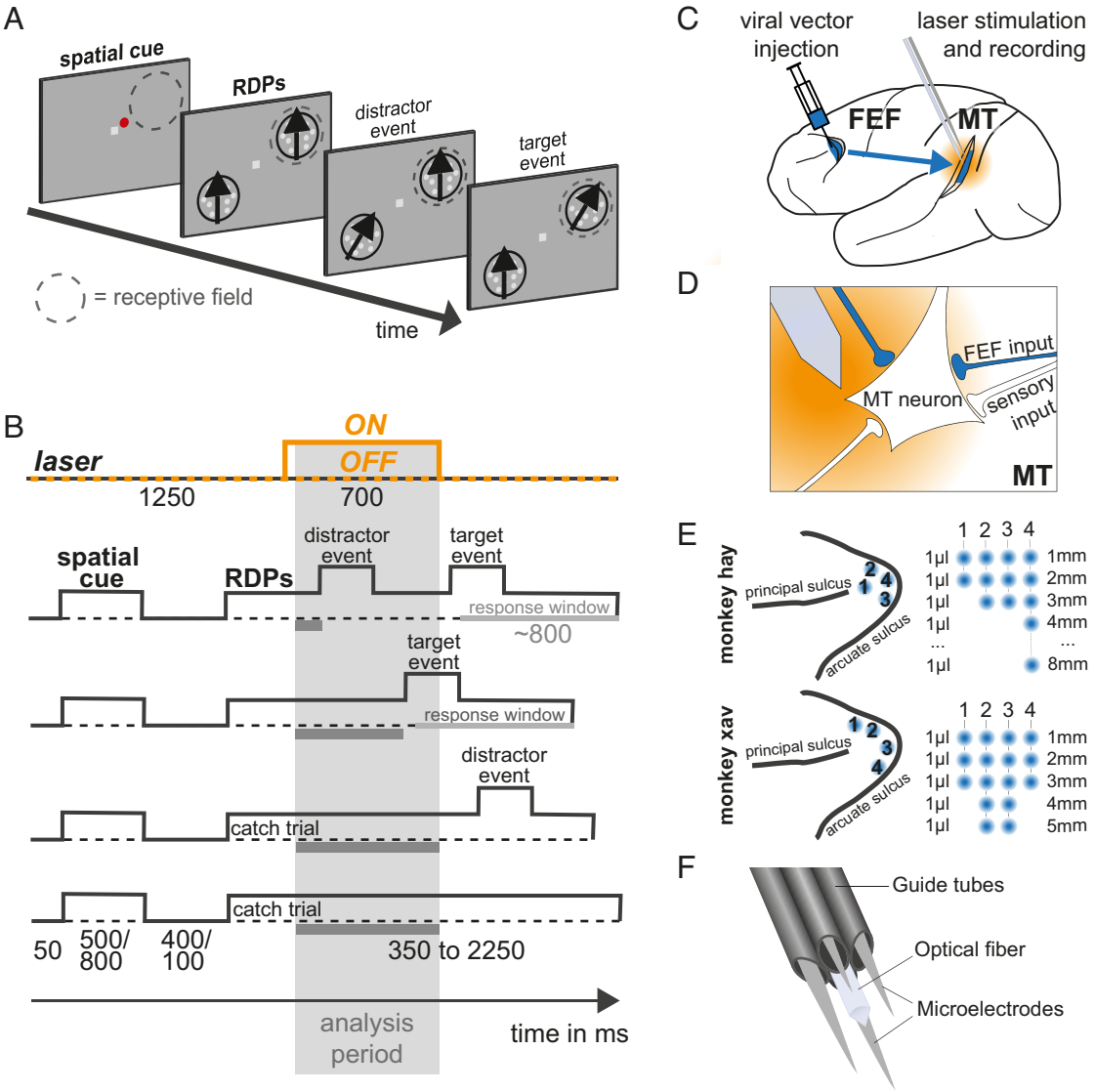

Fig. 1. (*A*) Spatial attention task design. A central cue was shown next to the fixation point, indicating to the monkeys to which of the two RDPs they had to respond. Subsequently, two RDPs appeared on the screen, one in the receptive field of the recorded neuron. The animals had to release a sensor as a response to a direction change in the cued RDP while ignoring direction changes in the uncued RDP. Our highly trained animals achieved a high hit rate, but despite the specific laser effects on local neuronal responses we observed, the behavioral performance was not significantly affected by the laser stimulation. This is likely because our paradigm is designed to maximize neural effects of spatial attentional modulation but is less behaviorally challenging than designs using spatially close or even overlapping stimuli (see the main text for details). (*B*) Time course of the spatial attention task. The spatial cue was shown for 500 or 800 ms and, after a period of 400 or 100 ms in which only the fixation point was presented, was followed by the display of the RDPs. The direction changes could happen at any time between 350 to 2,250 ms after RDP onset. Either one or no distractor event happened before the target event. In around 1/6 of trials, there was no change in the target RDP and the animals were rewarded for not releasing the sensor. After a direction change in the cued RDP, the animals had a response window of around 800 ms to release the button. In trials with laser stimulation, the laser stimulation started 300 ms after RDP onset and lasted for 700 ms or in case of an earlier target event ended with the target event. (*C*) Illustration of the experimental design. The viral vector was injected in area FEF. Laser stimulation and single-cell recordings were conducted in area MT. (*D*) Laser stimulation in area MT. Laser stimulation was conducted in area MT to inhibit the incoming input from FEF to MT while leaving sensory (and other) input to MT unchanged. The illustration shows the optical fiber (gray), an MT neuron, and four axon terminals targeting the neuron. The blue-colored axons contain opsins within their membrane and are inhibited by laser stimulation, while the white-colored axons are unaffected by laser stimulation. (*E*) FEF injection locations in monkeys hay and xav. One microliter of viral vector solution was injected at several depths (*Right* panel) at each of the four injection sites (*Left* panel, blue circles). The *Right* panel shows the injection depths for each injection site. For monkey hay, the maximum injection depths at the four injection sites were 2 mm, 3 mm, 3 mm, and 8 mm. For monkey xav, the maximum injection depths were 3 mm, 5 mm, 5 mm, and 3 mm. Injection sites were separated by 1 mm in depth. (*F*) Arrangement of microelectrodes and optical fiber within the concentrically arranged guide tubes. They were all independently movable. The optical fiber was placed in the central guide tube; up to four microelectrodes were placed in the surrounding guide tubes.

having a waveform duration shorter than 250 ms (putative inhibitory neurons) and 46 of 115 (40%) having a waveform duration longer than 250 ms (putative excitatory neurons). We found no significant difference in the attentional modulation without laser stimulation between these two groups of neurons (Wilcoxon rank-sum test, $P = 0.77$). The median attentional enhancement for the neurons with a short waveform was 19% (AMI: 0.085), and the median attentional enhancement for the neurons with a long waveform was 19% (AMI: 0.087). Laser stimulation reduced the attentional enhancement of neurons with a short waveform to 13% (AMI: 0.061, Wilcoxon signed-rank test, $P < 0.01$) and for neurons with a long waveform, although not significantly, also to 13% (AMI: 0.059, Wilcoxon signed-rank test, $P = 0.13$).

Effect of Laser Stimulation on General Firing Rate. Instead of affecting only the attentional modulation of firing rates in visual areas, FEF could also influence overall firing rates independent of the attentional state of the animal. Several studies suggest

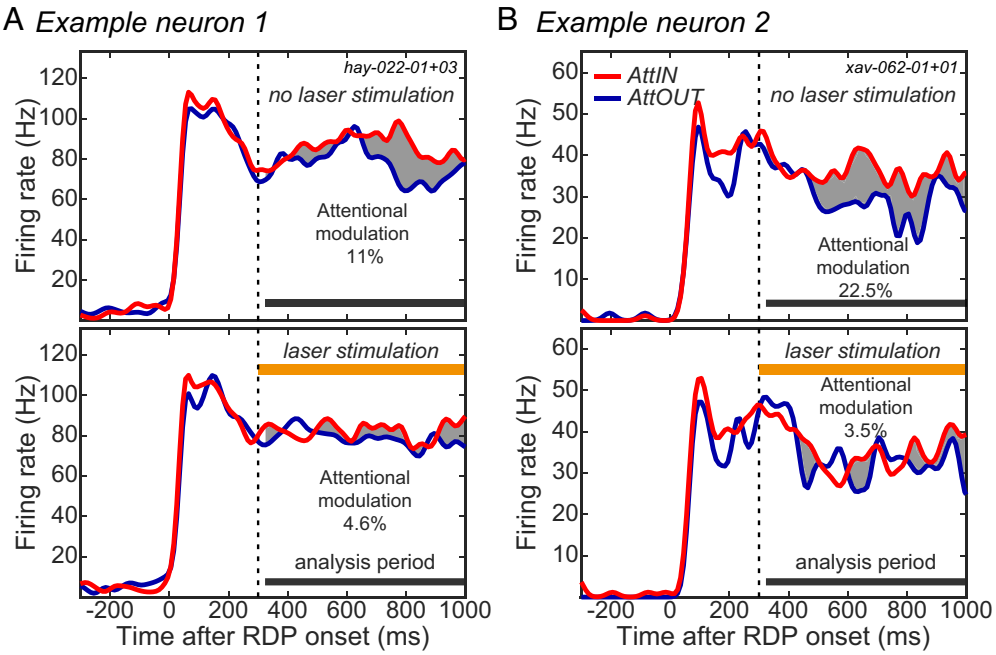

Fig. 2. Time course of firing rates in the AttIN (red) and AttOUT (blue) condition without and with laser stimulation. Laser stimulation started 300 ms after RDP onset and lasted until 1,000 ms after RDP onset (orange bar). We used the period of 320 ms after RDP onset until 1,000 ms after RDP onset (gray bar) as analysis window for the computation of mean firing rate, attentional modulation index, and laser stimulation index. (*A*) Example neuron showing a decrease in attentional modulation from 11% without laser stimulation to 4.6% with laser stimulation. (*B*) Example neuron showing a decrease in attentional modulation from 22.5% without laser stimulation to 3.5% with laser stimulation.

that laser stimulation alone can induce a change in firing rate by heating the tissue (45, 46). Owen and colleagues (46) found a suppression of firing rates with laser stimulation in mice, which was stronger in cortical fast-spiking cells than pyramidal cells. Therefore, we looked at the effect of laser stimulation on overall firing rates pooled across the attentional task conditions. Our analysis revealed no significant effect of laser stimulation on the overall firing rates (mean firing rate without laser stimulation: 64.1 Hz ± SEM 3.3 Hz, with laser stimulation 64.8 Hz ± SEM 3.3 Hz; Wilcoxon signed-rank test: $P = 0.07$). Similarly, we did not find any difference in the effect of laser stimulation on overall firing rates for narrow-spiking and broad-spiking neurons (mean firing rate: narrow-spiking neurons without laser stimulation 65.3 Hz ± SEM 4.7 Hz, with laser stimulation 65.5 Hz ± SEM 4.8 Hz, Wilcoxon signed-rank test: $P = 0.53$; broad-spiking neurons without laser stimulation 64.6 Hz ± SEM 5.3 Hz, with laser stimulation 65.4 Hz ± SEM 5.3 Hz, Wilcoxon signed-rank test: $P = 0.16$).

Effects of Laser Stimulation on Behavioral Performance. The animals in our study were highly trained and experienced in performing the spatial attention task. Even though our behavioral task was not designed to be sensitive to small changes in behavioral performance, we compared the animals' behavioral performance within all recording sessions (n = 137) between trials without and with laser stimulation (noLaser and laser), separately for the two attention conditions. We found no significant modulation of performance: The mean hit rate in the AttIN condition was not significantly changed by laser stimulation (noLaser: 75.7% ± SEM 0.9%, laser: 75.8% ± SEM 0.8%, Wilcoxon signed-rank test $P = 0.84$). The percentage of false alarms and misses was not significantly different between the stimulation conditions (false alarms: noLaser 11.9% ± SEM 0.5%, laser 11.7% ± SEM 0.5%; misses: noLaser 12.3% ± SEM 0.6%, laser 12.5% ± SEM 0.6%; Wilcoxon signed-rank test $P = 0.41$). Mean reaction times showed no significant difference with laser stimulation (noLaser: 389.2 ms ± SEM 3.6 ms, laser: 387.8 ms ± SEM 3.4 ms, Wilcoxon signed-rank test, $P = 0.37$). In the AttOUT condition, stimulation had no significant effect on the mean hit rate (noLaser: 75.2% ± SEM 0.8%, laser: 75.8% ± SEM 0.8, Wilcoxon signed-rank test $P = 0.15$), and the percentage of false alarms and misses was not significantly different between stimulation conditions (false alarms: noLaser 11.9% ± SEM 0.5%, laser 11.6% ± SEM 0.5%; misses: noLaser 12.9% ± SEM 0.6%, laser 12.7% ± SEM 0.6%; Wilcoxon signed-rank test $P = 0.63$). Mean reaction times were not significantly affected by laser stimulation (noLaser: 384.9 ms ± SEM 2.6 ms, laser: 387.4 ms ± SEM 2.7 ms, Wilcoxon signed-rank test $P = 0.34$).

Discussion

We selectively inhibited the direct input from prefrontal area FEF to extrastriate area MT in two rhesus macaques while they performed a spatial attention task. This selective inhibition was achieved by injecting a viral vector, containing the sequence of an inhibitory opsin, into FEF and a subsequent local laser stimulation in area MT to reduce the FEF's influence on MT neurons. Our results show a reduction of the attentional modulation of MT neurons by about one third, without affecting sensory response components. FEF, thus, specifically contributes to the attentional component of firing rates in area MT via its direct axonal projection to area MT. Our results contribute to an understanding of the important role of cortical feedback connections, complementing other studies for a causal manipulation of such projections (47–50).

The Role of FEF within the Global Attentional Network. The magnitude of reduction in attentional modulation we observed is likely an underestimation of the contribution of the direct FEF input to the attentional modulation in MT because our FEF viral injections almost certainly did not maximally transduce all FEF projections to MT and the laser stimulation similarly did not

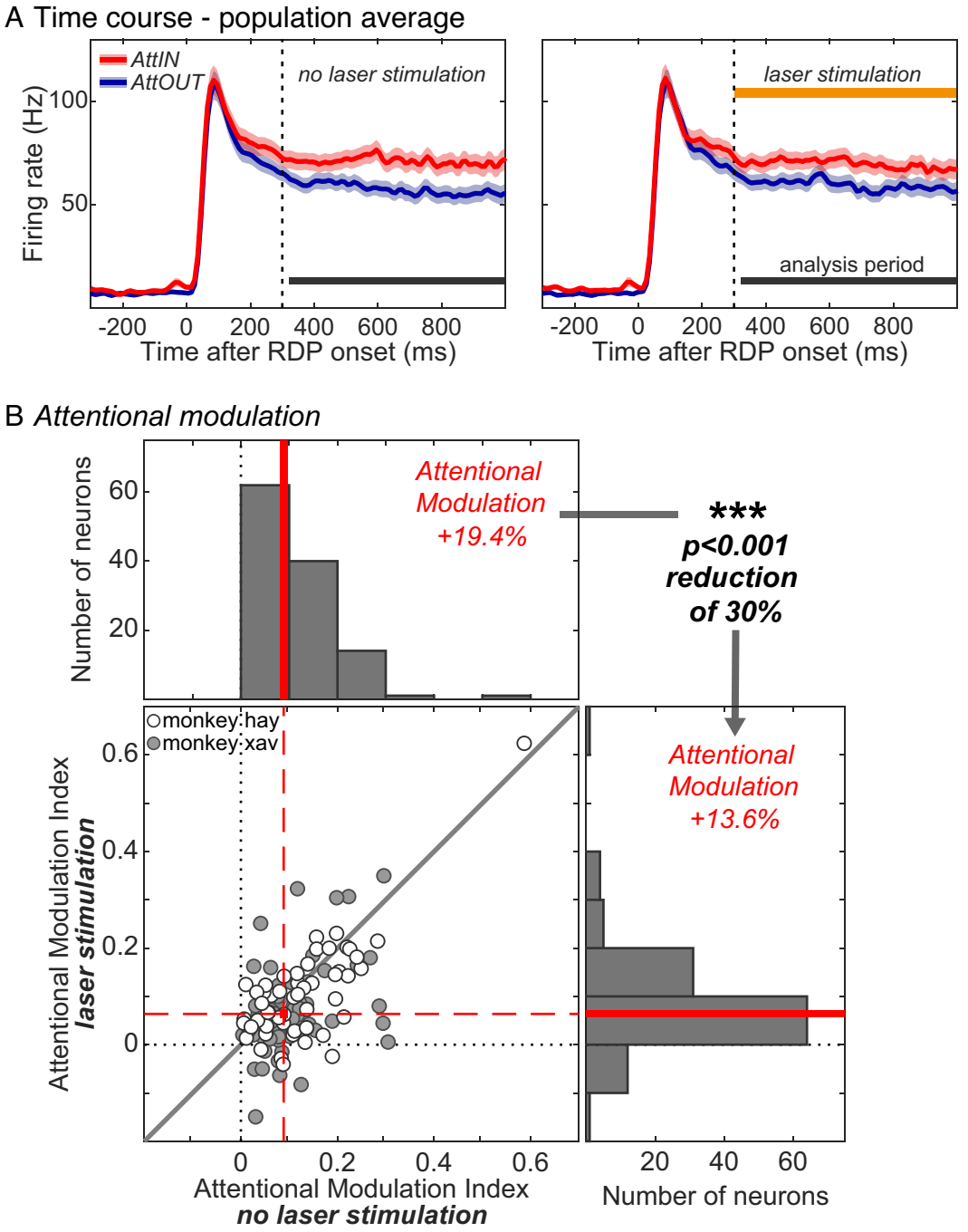

Fig. 3. (*A*) Time course. Population average across all neurons included in the analysis (n = 118). Time course of firing rates in the AttIN (red) and AttOUT (blue) condition without and with laser stimulation. Laser stimulation started 300 ms after RDP onset and lasted until 1,000 ms after RDP onset (orange bar). We used the period of 320 ms after RDP onset until 1,000 ms after RDP onset (gray bar) as analysis window for the computation of attentional modulation index and laser stimulation index. (*B*) Attentional modulation index (AMI) without and with laser stimulation is plotted for each neuron individually (bottom left plot; gray dots: monkey xav, white dots: monkey hay). The red, dashed line shows the median AMI for the two laser conditions. The diagonal black line marks theoretical equal values without and with laser stimulation. The histograms show the distributions of the attentional indices and the median value for the two laser conditions (red line). Median attentional modulation is given as a percentage.

completely deactivate all FEF inputs to a given MT neuron. Nevertheless, the reduction of the attentional modulation we found in MT is similar in magnitude to the reduction found in area V4 of macaques in a previous study, in which the prefrontal cortex of one hemisphere was extensively lesioned. This reduced the attentional modulation of firing rates in V4 by about 40% (29). Together with our study, these results confirm a causal role of FEF in the attention modulation of firing rates in both the ventral and dorsal cortical visual pathways. The observation that even an extensive lesion only results in a partial reduction in attentional modulation suggests that additional causal sources outside the prefrontal cortex exist. In addition, the results indicate that indirect pathways from the FEF to ipsilateral sensory areas play a small role, if any, in the attentional modulation.

A few areas have been suggested to play key roles in guiding spatial attention and could be additional causal sources for the attentional modulation in the visual cortex: the subcortical superior colliculus, the thalamic pulvinar nucleus, and cortical areas LIP. However, their causal contribution remains speculative, as no study has found a causal role for any of them in the attentional

modulation of firing rates in visual areas. It is assumed that neuromodulators, originating from axonal projections of neurons located in the brainstem, play a central mechanistical role in orchestrating attentional modulation. The three main candidates are acetylcholine, dopamine, and noradrenaline (51). Given the complexity with which the neurotransmitters interact and guide the attentional processes in various cortical areas, it is, however, challenging to estimate each transmitter's role in attention modulation. In area MT, the application of both cholinergic agonists and antagonists did not change the attentional modulation of firing rates (38).

Target Enhancement vs. Distractor Suppression. We found that firing rates were on average decreased with laser stimulation when attention was directed to the receptive field, while firing rates were increased when attention was directed away from the receptive field. That means that intact input from the FEF during attention results in a push–pull effect on firing rates: It increases firing rates of neurons when the focus of attention lies in their receptive field (target enhancement), and it decreases firing rates when the focus of attention lies elsewhere, such as in the other visual hemifield (distractor suppression). Results of previous studies in nonhuman primates have indicated that attention can enhance target processing (52), suppress distractor processing (39, 53), or act as a combination of both (54). Our results indicate that the neural architecture for target enhancement and distractor suppression is at least partly the same and not implemented via independent mechanisms (as suggested, e.g., in Chelazzi et al. 55). This is in line with a previous study, in which overlapping neuronal populations in the FEF have been shown to contribute to target selection and distractor suppression (56).

Effect on Behavioral Performance. Our data show no effect of inactivation of FEF input on behavioral performance. This likely is the result of several factors. For one, our experiment used a target and distractor in opposite visual hemifields. While this is well suited to maximize neural effects of spatial attentional modulation, it is less behaviorally challenging than designs using spatially close or even overlapping stimuli (57, 58). In addition, the laser stimulation was optimized for a local effect on the single neuron recorded from rather than to target the whole population of neurons contributing to the perceptual performance.

Ruling Out Alternative Explanations. There are two possible scenarios that need to be discussed as alternative causes for our results: laser stimulation of retrogradely transduced neurons and heat effects caused by laser stimulation. MT neurons projecting to area FEF could have taken up the viral vector via their axons and terminals in the FEF. We have previously shown (36) that this happens only very rarely (the density of retrogradely transduced neurons ranged from 0.52 to 1.62 neurons per mm^2). Furthermore, under such circumstances, our MT laser stimulation would modulate MT responses regardless of the behavioral condition and could thus not account for the specific effect on the attentional modulation we observe. Previous studies have shown that laser stimulation can change neural firing rates by heating of the tissue surrounding the optical fiber tip (45, 46). This is unlikely to be the basis of our findings since we have used a laser wavelength (594 nm) higher than those previously documented to evoke heating effects on firing rates (46) and expected to cause less heating (45). Furthermore, we have used optical fibers with a conical tip shape, which distribute the light more broadly, in contrast to the focused cylindrical light distribution of blunt fiber tips. Most importantly, heating should affect neurons independent from the attentional state of the animal. Pooling across our two attention conditions we find no change of overall firing rates with laser stimulation. Instead, our data show an increase of firing rates in the AttOUT condition and a decrease of firing rates in the AttIN condition. It is conceivable that optogenetic activation of neurons in the visual cortex results in phosphene-like effects, influencing the perception of stimuli at the corresponding retinotopic position and possibly triggering attentional shifts toward that location. We avoided such potential confounds by using inhibitory opsins, preventing sensory-like activations.

Effect of FEF Input onto Different Cell Types. Our recorded population of MT neurons consists of around 55% putatively inhibitory and 40% excitatory neurons, which we classified based on whether their spike waveform duration was shorter than 250 ms (narrow-spiking) or longer than 250 ms (broad-spiking). This proportion of cell types is similar to the proportion reported in a previous study (59). The two types of MT neurons did not show any difference in general firing rate, attentional modulation, or in the effect of laser stimulation on the attentional modulation in our recorded population of neurons. This is in contrast to what previous studies have reported for V4 (41, 43), where narrow-spiking and broad-spiking neurons showed a difference in their firing rates at least in the input layer of V4.

Conclusion. Our results show that the optogenetic inhibition of direct FEF input specifically reduces the attentional modulation of MT neurons, without affecting their sensory response component. We find that the direct FEF pathway to MT contributes to both the enhanced processing of a target stimulus and the suppression of distractor processing. Our study thus identifies the FEF as a core component of the attentional network. FEF neurons directly and specifically exert attentional top–down influence on sensory areas, differentially mediating the enhancement of attended and the suppression of unattended stimulus representations.

Methods

Animals. Two male monkeys (*Macaca mulatta*; 19 and 12–13 y) weighing 11–14 kg were part of this study. The animals were group-housed in an animal facility of the German Primate Center (DPZ). They were exposed to the natural day/night circle through windows and access to an outdoor cage. The facility provides the animals with an enriched environment including a multitude of toys and wooden structures, natural as well as artificial light. Each group was kept in a large enclosure, exceeding the size requirements of the European regulations, including access to outdoor space and in visual and auditory interaction with the animals in two other enclosures. Both monkeys had ample access to dry food and received additional fresh fruits and vegetables, as well as protein-containing insects, cereals, nuts, or yogurt. During the training and recording days, they gained most of their fluid intake by juice reward during the experiment. The juice was chosen according to the animal's preference and usually switched from day to day between the most preferred juices. The animals worked as long as they wanted. Whenever no training or recording was conducted, they had free access to water and dry food and got additional fresh fruits and vegetables. The animals' psychological and veterinary welfare was monitored by the DPZ's staff veterinarians, the animal facility staff, and the lab's scientists, all specialized in working with nonhuman primates. We have established a comprehensive set of measures to ensure that the severity of our experimental procedures falls into the category of mild to moderate, according to the severity categorization of Annex VIII of the European Union's directive 2010/63/EU on the protection of animals used for scientific purposes (60). All animal work and housing is conducted in accordance with all applicable German and European regulations. The scientists in this study are aware of and are committed to the great responsibility they have in ensuring the best possible science with the least possible harm to any animals used in scientific research (61, 62). All animal procedures have been approved by the responsible regional government [Niedersaechsisches Landesamt fuer

Verbraucherschutz und Lebensmittelsicherheit (LAVES), Oldenburg, Germany] under the permit number 3392 42502-04-13/1100. All surgical and imaging procedures were done under appropriate anesthesia, with appropriate analgesics and in accordance with German laws governing animal use.

Implants. Monkey hay had been implanted with a titanium headpost before the current study, in the context of contributing to earlier attention studies. A cylindrical recording chamber was mounted to provide access to a craniotomy above area MT of the left hemisphere at the initiation of the current study. Monkey xav was implanted with a titanium headpost and a recording chamber above area MT of the right hemisphere. He did not participate in any other attention or electrophysiological study before.

Viral Vector Injection. Viral vector injection was conducted during surgery. We determined the location and the shape of the FEF of both animals based on a prior MRI scan and by anatomical landmarks (i.e., the arcuate and principal sulcus) after dura opening. A viral vector (AAV5-aCamKII-eNpHR3.0-mCherry, UNC Vector Core, titer: 4.7×10^{12} vg/mL; same batch for both animals) was injected into the left FEF of monkey hay and the right FEF of monkey xav. We used a Hamilton syringe (25 µL, 32-gauge needle with sharpened tip) to make four penetrations (Fig. 1*C*). The distance between two penetrations was approximately 1.5 to 2 mm. At each penetration, we injected at multiple depths. An extended histological analysis of opsin expression 2 y after viral vector injection in monkey hay can be found in ref. 36. In monkey hay, we injected 1 µL every mm with a speed of 200 nL/s. Starting with the deepest injection, we waited 5 min after each microliter to retract the tip of the syringe to the next depth. In monkey xav, we injected 1 µL every mm with a speed of 300 nL/s and waited 2 to 5 min before retracting the syringe to the next depth. The exact spatial configuration of the four penetrations was dependent on individual anatomy and the localization of blood vessels. Therefore, the configuration differed between the two monkeys (Fig. 1*C*). We could not record neural responses in area FEF in our animals. Therefore, we aimed at transducing as many FEF cells as possible to target as many of the FEF feedback projections to area MT as possible.

Recordings and Stimulation. Stimulation experiments started several months after the injection (see *SI Appendix*, Fig. S1 for distribution of time between injection and recordings). We recorded single-cell responses in area MT while optically stimulating in the vicinity of the electrode tip. Since area MT lies deep within a sulcus, we have neither information in which layer the recorded neurons were located nor about which layers of MT we stimulated with the laser. Area MT was localized by an anatomical MRI scan, and our recording sites were chosen based on the MRI scan, as well as the presence of a majority of direction-tuned cells. Prior to recording, we determined the position of the receptive field and the preferred direction of the isolated neuron by hand mapping, using a random dot pattern (RDP) moving with an aperture, whose direction and position was controlled by a computer mouse. If the preferred direction was not apparent with the hand mapping, we systematically presented different stimulus directions in the receptive field of a neuron and determined the preferred direction based on an online analysis of the firing rate.

We used a multielectrode manipulator (20-channel tetrode Mini Matrix System, Thomas Recording) with a concentric arrangement of five guide tubes for our recordings: a circle of four guide tubes surrounded a central guide tube. The central guide tube contained an optical fiber (diameter 120 µm, conical tip, Thomas Recording) while the surrounding ones each contained a microelectrode (Fig. 1*D*). The optical fiber was coupled to an orange (594 nm) diode-pumped solid-state (DPSS) laser (Cobolt AB) by an optical patch cable (105 µm, NA 0.22, Thorlabs, stainless steel tubing with black plastic sheath). The laser power was controlled by an acousto-optical modulator (AOM). The AOM and the experiment were controlled by the open-source software Mworks (mworks-project.org, version 0.6) running on an iMac (Apple Inc.). Neural data were recorded with an Omniplex system (Plexon Inc.) with a sampling rate of 40kHz. Spikes were sorted online and resorted or verified offline using the software Plexon OfflineSorter (version 3.3.5); except for 2 units for which we used the online sorted spikes due to technical issues with the data files. The eye position was monitored with a video-based eye tracker (EyeLink 1000, SR Research).

Before each recording session, we measured the light power at the end of the optical fiber tip with a power meter (PM100D, photodiode power sensor S121C, Thorlabs). We used each optical fiber repeatedly in several sessions but exchanged them whenever a major change in the light power at the tip occurred or when the glass body showed any sign of damage. We used a laser power that resulted in a measurable light power of 14 mW or 16 mW at the fiber tip (these values were based on the maximum laser power reported in (63)). Each optical fiber was usually used on several days without showing a considerable change in the maximum output power. The optical fibers never broke as a result of the recordings. They had a sharpened tip, which resulted in an approximately circular light distribution around the tip (Thomas Recording, fiber type: VIS 400 nm–900 nm, NA = 0,86, EFL4188, borosilicate glass, fiber outer diameter: 120 µm, tip shape: D). The power measured straight at the tip was usually higher than the laser power measured at the flanks of the tip. The tip length and shape differed slightly from fiber to fiber and therefore also the light distribution. We adapted the laser power for each recording session so that the light power coming out straight at the tip was constant. The optical fiber tip was placed above the tip of the recording electrode during the recordings for a majority of recordings. For a few recordings, the optical fiber tip was lower than the electrode tip. We used variable vertical distances of −350 to 850 µm between the two tips (*SI Appendix*, Fig. S1). They were the result of practical difficulties in keeping a cell isolated while placing the optical fiber tip at a certain distance to the electrode tip.

Behavioral Task. The animals were conducting a spatial attention task (Fig. 1*A*). A red (size 0.2 × 0.2dva) fixation point was shown in the center of a computer monitor (BenQ XL2720T, resolution 1,920 × 1,080, refresh rate 120 Hz). The animals had to foveate it and touch a proximity sensor (Carlo Gavazzi EC3016-NPAPL) in front of them to start a trial. A red circular cue (radius 0.3dva) appeared on the screen next to the fixation point after 50 ms (see Fig. 1*B* for time course). The cue instructed the monkeys, which of the two subsequently presented moving random dot pattern (RDP) was the target stimulus.

The cue was shown for 500 ms (or 800 ms for the initial recordings in monkey xav) and followed by a blank period with only the fixation point present for 400 ms (or 100 ms for the initial recordings of monkey xav). After that, two RDPs appeared, one in the receptive field of the recorded neuron and the other with the maximum distance at the same eccentricity in the opposite visual field. This design generated two attention conditions: The monkeys were either attending to the stimulus inside the receptive field (AttIN) or to the stimulus outside of the receptive field (AttOUT).

The size of the RDPs was adapted manually to cover approximately the most responsive part of the receptive field. We used a motion direction pool of eight directions (0°, 45°, 90°, 135°, etc.). For each neuron, we either recorded a full set of eight directions or only two directions (one out of the two directions was closest to the preferred direction, and the other direction was 180° apart). For some recording sessions, we started with two directions and continued with eight directions after enough repetitions had been recorded for all conditions. Trials with and without laser stimulation, the two or eight movement directions, and the two possible target locations were pseudorandomly chosen. This resulted in 2 × 2 × 2 conditions or 2 × 8 × 2 conditions per recorded neuron. The monkeys had to respond to a direction change which was fixed for each recording session, but ranging in magnitude from 20° to 45° (except for two sessions with a change magnitude of 90°) in the target stimulus by releasing the proximity sensor. A direction change in the noncued stimulus had to be ignored. In nine sessions, the direction change magnitude was changed within the specified range of magnitudes (in six sessions increased; in three sessions decreased) throughout the experiment because the stimulus configuration (RF location and size) seemed to be too easy or difficult for the monkey. In general, the size of the change was chosen to ensure a sufficient engagement of the animal but large enough to allow for a high hit rate across a recording session. It is therefore likely that the task did not require the highest level of attention and correspondingly behavioral performance is not sensitive to small changes in attentional modulation.

The monkeys received juice for completing the trial correctly. Trials in which the monkey released the sensor too early (false alarms) or did not release it after a target event (misses) were not rewarded. Up to two direction changes could occur in one trial, but never within the same RDP. 1/6 of the trials were catch trials, in which no direction change occurred in the target stimulus (but could occur in the distractor RDP). In this case, the animals had to hold the proximity sensor until they received a reward. Monkey hay was using his left hand for the task, while monkey xav was using his right hand.

We stimulated with a continuous laser pulse of 700 ms during a period of stimulus presentation in which we expected attentional modulations of firing rates, i.e.,

starting 300 ms after the onset of the two moving RDP. Trials with and without laser stimulation were randomly interleaved, generating two stimulation conditions (noLaser and laser). The direction changes happened between 350 ms and 4,300 ms after onset of the two RDPs and lasted for 250 ms (monkey hay) or 180 to 250 ms (monkey xav). The animals had a response window of around 800 ms (variable across sessions: 750–840 ms, but fixed for each session). If they did not respond within this window, a warning sound was played and the trial was not rewarded.

Data analysis. We included neurons in our analysis if they were well isolated, responded to our visual stimuli, showed direction selectivity, and if the animal's behavior allowed for the recording of neuronal responses throughout the time period used for the laser stimulation for every condition. All data were analyzed with Matlab (R2020b) using custom-written scripts. We only analyzed hit trials, i.e., trials in which the sensor was released in response to a direction change in the target stimulus and trials in which the sensor was hold until the trial ended without a direction change in the target stimulus. The data underlying this manuscript is available in a public data repository (64).

Computation of firing rates. Firing rates were computed based on a PSTH with a bin width of 10 ms. Trials had different lengths due to the randomization of the time point of direction change. The analysis of a trial ended with a direction change either in the distractor or the target stimulus. For trials without a direction change, the analysis ended 30 ms before the animal got the juice reward. We calculated the firing rates for the time period of 320 to 1,000 ms after RDP onset, which was the laser stimulation period. We started 20 ms after potential laser onset to account for a delay in laser effects on opsins and consequent hyperpolarization of the axons. Due to the different lengths of the trials, we obtained fewer repetitions for late compared to early time points within the analysis period.

Determination of preferred direction. We determined the preferred direction of a neuron based on the firing rate in the AttIN condition without laser stimulation within the analysis window. For neurons that were recorded with only two directions, the preferred direction was determined online during the recording and was verified offline. For neurons that were recorded with eight directions, we determined the preferred direction by first calculating the mean firing rate for each direction in the AttIN condition without laser stimulation and then fitting a van Mises function to the data if there were enough repetitions for at least five directions. Given our fixed set of eight directions, we chose the recorded direction that was closest to the preferred direction determined by the fit. In rare cases, we did not record enough repetitions for the direction closest to the fitted preferred direction and chose the neighboring direction as the preferred if the peak of the tuning curve was located in between these two directions. We only used the trials in which the preferred direction was shown for the following analysis steps.

Time course of firing rates and attentional modulation. For visualization of the time course of firing rate, we convolved the discrete firing data with a Gaussian kernel ($\sigma = 20$ ms for the example neurons; $\sigma = 10$ ms for the population average). The attentional modulation index (AMI) was calculated by the following formula:

$$AMI = \frac{(FR_{AttIN} - FR_{AttOUT})}{(FR_{AttIN} + FR_{AttOUT})}.$$

We calculated the AMI for each neuron independently for trials without laser stimulation and with laser stimulation. Neurons in which the AMI was negative without laser stimulation were excluded from further analysis because they did not fulfill our basic assumption of a higher firing rate when attention was directed to the receptive field. This was true for 20 out of 138 neurons. The median attentional modulation in percentage was calculated from the median attentional modulation index by the formula:

$$AMI_{percentage} = 2x\frac{AMI}{1 - AMI}x100.$$

Effects of laser stimulation on target and distractor processing. To determine how laser stimulation affects firing rates in the two attention conditions, we calculated a laser stimulation index (LSI) for each neuron analogously to the attentional modulation index and separately for the two attention conditions:

$$LSI = \frac{(FR_{laser} - FR_{noLaser})}{(FR_{laser} + FR_{noLaser})}.$$

A positive LSI value means that firing rates were increased by laser stimulation, while a negative LSI value shows a decrease; we report the values as percentages calculated via the same formula as the attentional modulation.

Classification of neuronal cell type based on waveform duration. Waveforms were extracted with the help of the Plexon OfflineSorter (version 3.3.5) and plotted and analyzed with Matlab (2020b). Waveforms were averaged across spikes. We included all spikes within a recorded file independent of whether they occurred during or outside of a trial. Waveform duration was determined as the duration from minimum to a subsequent maximum voltage. We plotted the distribution of waveform duration and tested for bimodality with a Hartigan's dip test (65). *P* values smaller than 0.5 indicate significant multimodality, while *P* values between 0.05 and 0.1 indicate multimodality with marginal significance (59, 66). We classified cells as narrow-spiking if their waveform duration was smaller than 250 ms and as broad-spiking if their waveform duration was larger than 250 ms. Neurons with a waveform equal to 250 ms were left unclassified. Two neurons were not included in the waveform analysis due to technical issues with the Plexon data file, and 1 neuron was not included because the waveform shape indicated that it originated from two separate units.

Effect of laser stimulation on general firing rate. We determined whether the laser stimulation had a general impact on firing rates by calculating the average firing rate across all trials independent of attention condition and compared trials without and with laser stimulation.

Effects of laser stimulation on behavioral performance. The hit rate was determined as the percentage of trials in which either the direction change was correctly detected by a button release or the button was held until a reward was given in the catch trials (in which no direction change occurred in the target RDP). Reaction times were calculated based on trials in which a direction occurred in the cued stimulus. Trials with fixation breaks were excluded from the analysis and not counted as error trials, likewise were the trials in which a button release occurred before the potential laser stimulation period. We calculated the performance based on all recording sessions and including all trials independent of stimulus directions.

Data, Materials, and Software Availability. Additional data have been deposited in GRO (https://data.goettingen-research-online.de/dataset.xhtml?persistentId=doi:10.25625/PGJZS8) (64).

ACKNOWLEDGMENTS. We are grateful to the veterinary and the animal husbandry staff of the DPZ for their care of the animals, to Ralf Brockhausen, Leonore Burchardt, Klaus Heisig, Janine Kuntze, Sina Plümer, and Dirk Prüsse for expert technical assistance, to Jens Gruber and Lara-Timantra Schiller for viral vector testing and handling, and to Alexander Gail, Hansjörg Scherberger, Michal Fortuna, and Hao Guo for collaboration in implementing optogenetic experiments. A special thanks to Jochen F. Staiger for providing guidance in conducting histology of the brain tissue and testing the viral vector. We thank the UNC vector core for viral packaging and Karl Deisseroth for viral constructs. The study was funded by the Leibniz Association (WGL SAW-2014-DPZ-1) and the German Research Foundation (Deutsche Forschungsgemeinschaft, DFG: CRC 889 Cellular mechanisms of sensory processing; project C04). Portions of the paper were developed from the thesis of J.H.

1. K. Clark, R. F. Squire, Y. Merrikhi, B. Noudoost, Visual attention: Linking prefrontal sources to neuronal and behavioral correlates. *Prog. Neurobiol.* **132**, 59–80 (2015).
2. I. C. Fiebelkorn, S. Kastner, Functional specialization in the attention network. *Annu. Rev. Psychol.* **71**, 221–249 (2020).
3. B. Wild, S. Treue, Primate extrastriate cortical area MST: A gateway between sensation and cognition. *J. Neurophysiol.* **125**, 1851–1882 (2021).
4. T. Womelsdorf, S. Everling, Long-range attention networks: Circuit motifs underlying endogenously controlled stimulus selection. *Trends Neurosci.* **38**, 682–700 (2015).
5. J. H. R. Maunsell, Neuronal mechanisms of visual attention. *Annu. Rev. Vis. Sci.* **1**, 373–391 (2015).
6. V. Mehrpour, J. C. Martinez-Trujillo, S. Treue, Attention amplifies neural representations of changes in sensory input at the expense of perceptual accuracy. *Nat. Commun.* **11**, 2128 (2020).
7. J. Moran, R. Desimone, Selective attention gates visual processing in the extrastriate cortex. *Science* **229**, 782–784 (1985).
8. S. Treue, J. H. Maunsell, Attentional modulation of visual motion processing in cortical areas MT and MST. *Nature* **382**, 539–541 (1996).

9. T. Moore, M. Fallah, Control of eye movements and spatial attention. *Proc. Natl. Acad. Sci. U.S.A.* **98**, 1273–1276 (2001).
10. T. Moore, K. M. Armstrong, Selective gating of visual signals by microstimulation of frontal cortex. *Nature* **421**, 370–373 (2003).
11. C. Wardak, G. Ibos, J.-R. Duhamel, E. Olivier, Contribution of the monkey frontal eye field to covert visual attention. *J. Neurosci.* **26**, 4228–4235 (2006).
12. C. Wardak, E. Olivier, J.-R. Duhamel, A deficit in covert attention after parietal cortex inactivation in the monkey. *Neuron* **42**, 501–508 (2004).
13. I. C. Fiebelkorn, M. A. Pinsk, S. Kastner, A dynamic interplay within the frontoparietal network underlies rhythmic spatial attention. *Neuron* **99**, 842–853.e8 (2018).
14. T. M. Herrington, J. A. Assad, Temporal sequence of attentional modulation in the lateral intraparietal area and middle temporal area during rapid covert shifts of attention. *J. Neurosci.* **30**, 3287–3296 (2010).
15. Y. B. Saalmann, I. N. Pigarev, T. R. Vidyasagar, Neural mechanisms of visual attention: How top-down feedback highlights relevant locations. *Science* **316**, 1612–1615 (2007).
16. P. F. Balan *et al.*, Fast compensatory functional network changes caused by reversible inactivation of monkey parietal cortex. *Cereb. Cortex* **29**, 2588–2606 (2019).
17. J. R. Müller, M. G. Philiastides, W. T. Newsome, Microstimulation of the superior colliculus focuses attention without moving the eyes. *Proc. Natl. Acad. Sci. U.S.A.* **102**, 524–529 (2005).
18. L. P. Lovejoy, R. J. Krauzlis, Inactivation of primate superior colliculus impairs covert selection of signals for perceptual judgments. *Nat. Neurosci.* **13**, 261–266 (2010).
19. A. Zénon, R. J. Krauzlis, Attention deficits without cortical neuronal deficits. *Nature* **489**, 434–437 (2012).
20. H. Zhou, R. J. Schafer, R. Desimone, Pulvinar-cortex interactions in vision and attention. *Neuron* **89**, 209–220 (2016).
21. I. C. Fiebelkorn, M. A. Pinsk, S. Kastner, The mediodorsal pulvinar coordinates the macaque fronto-parietal network during rhythmic spatial attention. *Nat. Commun.* **10**, 215 (2019).
22. J. C. Anderson, H. Kennedy, K. A. C. Martin, Pathways of attention: Synaptic relationships of frontal eye field to V4, lateral intraparietal cortex, and area 46 in macaque monkey. *J. Neurosci.* **31**, 10872–10881 (2011).
23. T. Ninomiya, H. Sawamura, K.-I. Inoue, M. Takada, Segregated pathways carrying frontally derived top-down signals to visual areas MT and V4 in macaques. *J. Neurosci.* **32**, 6851–6858 (2012).
24. G. B. Stanton, C. J. Bruce, M. E. Goldberg, Topography of projections to posterior cortical areas from the macaque frontal eye fields. *J. Comp. Neurol.* **353**, 291–305 (1995).
25. K. M. Armstrong, T. Moore, Rapid enhancement of visual cortical response discriminability by microstimulation of the frontal eye field. *Proc. Natl. Acad. Sci. U.S.A.* **104**, 9499–9504 (2007).
26. G. G. Gregoriou, S. J. Gotts, H. Zhou, R. Desimone, High-frequency, long-range coupling between prefrontal and visual cortex during attention. *Science* **324**, 1207–1210 (2009).
27. B. Noudoost, T. Moore, Control of visual cortical signals by prefrontal dopamine. *Nature* **474**, 372–375 (2011).
28. G. G. Gregoriou, S. J. Gotts, R. Desimone, Cell-type-specific synchronization of neural activity in FEF with V4 during attention. *Neuron* **73**, 581–594 (2012).
29. G. G. Gregoriou, A. F. Rossi, L. G. Ungerleider, R. Desimone, Lesions of prefrontal cortex reduce attentional modulation of neuronal responses and synchrony in V4. *Nat. Neurosci.* **17**, 1003–1011 (2014).
30. D. Veniero *et al.*, Top-down control of visual cortex by the frontal eye fields through oscillatory realignment. *Nat. Commun.* **12**, 1757 (2021).
31. T. R. Marshall, J. O'Shea, O. Jensen, T. O. Bergmann, Frontal eye fields control attentional modulation of alpha and gamma oscillations in contralateral occipitoparietal cortex. *J. Neurosci.* **35**, 1638–1647 (2015).
32. S. Tremblay *et al.*, An open resource for non-human primate optogenetics. *Neuron* **108**, 1075–1090.e6 (2020).
33. A. Galvan *et al.*, Nonhuman primate optogenetics: Recent advances and future directions. *J. Neurosci.* **37**, 10894–10903 (2017).
34. Y. El-Shamayleh, G. D. Horwitz, Primate optogenetics: Progress and prognosis. *Proc. Natl. Acad. Sci. U.S.A.* **116**, 26195–26203 (2019).
35. M. Oguchi, M. Sakagami, Dissecting the prefrontal network with pathway-selective manipulation in the Macaque Brain–A review. *Front. Neurosci.* **16**, 917407 (2022).
36. M. G. Fortuna *et al.*, Histological assessment of optogenetic tools to study fronto-visual and fronto-parietal cortical networks in the rhesus macaque. *Sci. Rep.* **10**, 11051 (2020).
37. S. Treue, J. C. Martínez Trujillo, Feature-based attention influences motion processing gain in macaque visual cortex. *Nature* **399**, 575–579 (1999).
38. V. K. Veith, C. Quigley, S. Treue, Cholinergic manipulations affect sensory responses but not attentional enhancement in macaque MT. *BMC Biol.* **19**, 49 (2021).
39. N. Malek, S. Treue, P. Khayat, J. Martinez-Trujillo, Distracter suppression dominates attentional modulation of responses to multiple stimuli inside the receptive fields of middle temporal neurons. *Eur. J. Neurosci.* **46**, 2844–2858 (2017).
40. S. Treue, Visual attention: The where, what, how and why of saliency. *Curr. Opin. Neurobiol.* **13**, 428–432 (2003).
41. J. F. Mitchell, K. A. Sundberg, J. H. Reynolds, Differential attention-dependent response modulation across cell classes in macaque visual area V4. *Neuron* **55**, 131–141 (2007).
42. M. Vinck, T. Womelsdorf, E. A. Buffalo, R. Desimone, P. Fries, Attentional modulation of cell-class-specific gamma-band synchronization in awake monkey area v4. *Neuron* **80**, 1077–1089 (2013).
43. A. S. Nandy, J. J. Nassi, J. H. Reynolds, Laminar organization of attentional modulation in macaque visual area V4. *Neuron* **93**, 235–246 (2017).
44. M. Dasilva *et al.*, Cell class-specific modulation of attentional signals by acetylcholine in macaque frontal eye field. *Proc. Natl. Acad. Sci. U.S.A.* **116**, 20180–20189 (2019).
45. J. M. Stujenske, T. Spellman, J. A. Gordon, Modeling the spatiotemporal dynamics of light and heat propagation for in vivo optogenetics. *Cell Rep.* **12**, 525–534 (2015).
46. S. F. Owen, M. H. Liu, A. C. Kreitzer, Thermal constraints on in vivo optogenetic manipulations. *Nat. Neurosci.* **22**, 1061–1065 (2019).
47. J. J. Nassi, S. G. Lomber, R. T. Born, Corticocortical feedback contributes to surround suppression in V1 of the alert primate. *J. Neurosci.* **33**, 8504–8517 (2013).
48. S. R. Debes, V. Dragoi, Suppressing feedback signals to visual cortex abolishes attentional modulation. *Science* **379**, 468–473 (2023).
49. J. M. Hupé *et al.*, Cortical feedback improves discrimination between figure and background by V1, V2 and V3 neurons. *Nature* **394**, 784–787 (1998).
50. L. Nurminen, S. Merlin, M. Bijanzadeh, F. Federer, A. Angelucci, Top-down feedback controls spatial summation and response amplitude in primate visual cortex. *Nat. Commun.* **9**, 2281 (2018).
51. D. E. L. Lockhofen, C. Mulert, Neurochemistry of visual attention. *Front. Neurosci.* **15**, 643597 (2021).
52. A. M. Ni, S. Ray, J. H. R. Maunsell, Tuned normalization explains the size of attention modulations. *Neuron* **73**, 803–813 (2012).
53. A. E. Ipata, A. L. Gee, J. Gottlieb, J. W. Bisley, M. E. Goldberg, LIP responses to a popout stimulus are reduced if it is overtly ignored. *Nat. Neurosci.* **9**, 1071–1076 (2006).
54. G. M. Ghose, J. H. R. Maunsell, Spatial summation can explain the attentional modulation of neuronal responses to multiple stimuli in area V4. *J. Neurosci.* **28**, 5115–5126 (2008).
55. L. Chelazzi, F. Marini, D. Pascucci, M. Turatto, Getting rid of visual distractors: The why, when, how, and where. *Curr. Opin. Psychol.* **29**, 135–147 (2019).
56. J. D. Cosman, K. A. Lowe, W. Zinke, G. F. Woodman, J. D. Schall, Prefrontal control of visual distraction. *Curr. Biol.* **28**, 414–420.e3 (2018).
57. D. R. Patzwahl, S. Treue, Combining spatial and feature-based attention within the receptive field of MT neurons. *Vision Res.* **49**, 1188–1193 (2009).
58. S.-A. Yoo, J. C. Martinez-Trujillo, S. Treue, J. K. Tsotsos, M. Fallah, Attention to visual motion suppresses neuronal and behavioral sensitivity in nearby feature space. *BMC Biol.* **20**, 220 (2022).
59. S. Torres-Gomez *et al.*, Changes in the proportion of inhibitory interneuron types from sensory to executive areas of the primate neocortex: Implications for the origins of working memory representations. *Cereb. Cortex* **30**, 4544–4562 (2020).
60. D. Pfefferle, S. Plümer, L. Burchardt, S. Treue, A. Gail, Assessment of stress responses in rhesus macaques (Macaca mulatta) to daily routine procedures in system neuroscience based on salivary cortisol concentrations. *PLoS One* **13**, e0190190 (2018).
61. P. R. Roelfsema, S. Treue, Basic neuroscience research with nonhuman primates: A small but indispensable component of biomedical research. *Neuron* **82**, 1200–1204 (2014).
62. S. Treue, R. N. Lemon, "The indispensable contribution of nonhuman primates to biomedical research" in *Nonhuman Primate Welfare: From History, Science, and Ethics to Practice*, L. M. Robinson, A. Weiss, Eds. (Springer, ed. 1, 2022) https://doi.org/10.1007/978-3-030-82708-3.
63. W. R. Stauffer *et al.*, Dopamine neuron-specific optogenetic stimulation in rhesus macaques. *Cell* **166**, 1564-1571 (2016).
64. S. Treue, Manuscript Data for Hueer, Saxena & Treue - PNAS - 2023. GRO.data. https://doi.org/10.25625/PGJZS8. Deposited 17 November 2023.
65. J. A. Hartigan, P. M. Hartigan, The dip test of unimodality. *Ann. Statist.* **13**, 70–84 (1985).
66. J. B. Freeman, R. Dale, Assessing bimodality to detect the presence of a dual cognitive process. *Behav. Res. Methods* **45**, 83–97 (2013).